

# Start-up of a Hybrid Loop Thermosyphon/Pulsating Heat Pipe on Ground and on board a sounding rocket

Mauro Mameli<sup>1\*</sup>, Stefano Piacquadio<sup>1</sup>, Alessandro Simone Viglione<sup>1</sup>, Andrea Catarsi<sup>1</sup>, Carlo Bartoli<sup>1</sup>, Marco Marengo<sup>2</sup>, Paolo Di Marco<sup>1</sup>, Sauro Filippeschi<sup>1</sup>,

<sup>1</sup>University of Pisa, Largo Lucio Lazzarino 2, 56122 Pisa, Italy

<sup>2</sup>School of Computing, Engineering and Mathematics, University of Brighton, Lewes Rd, Brighton BN2 4AT, United Kingdom

\* Corresponding author : [mauro.mameli@ing.unipi.it](mailto:mauro.mameli@ing.unipi.it), tel. +39 050 2217166

## Abstract

A large tube may still behave, to a certain extent, as a capillary in a micro-gravity environment. This very basic concept is here applied to a two-phase passive heat transfer device to obtain a new family of hybrid wickless heat pipes. Indeed, a Loop Thermosyphon, which usually consists of a large tube, closed end to end in a loop, evacuated and partially filled with a working fluid and intrinsically gravity assisted, may become a capillary tube in space condition and turn its thermo-fluidic behavior into a Pulsating Heat Pipe. This work presents the results obtained on such a hybrid device heated at 200 W both on board a sounding rocket (ESA REXUS 22, microgravity period ~120 s), and on ground in vertical and anti-gravity orientation. Since no steady state occurred in microgravity conditions, the comparison between flight and ground data focuses on the startup phenomenon, whereas the thorough ground test campaign describes the limits and performances of the device working in thermosyphon mode. The expected thermal behavior in microgravity conditions is between that of a purely conductive tube in anti-gravity conditions on ground and that of a gravity assisted thermosyphon. Since a microgravity period of approximately 120s is not sufficient to reach a pseudo steady state regime, further investigation on a longer-term weightless condition is mandatory.

*Keywords:* Pulsating Heat Pipe; Space; Sounding rocket; Startup;

## 1 INTRODUCTION

Spacecrafts thermal control subsystems require high standard components for heat transfer. Moreover, the continuously increasing trend for electronics miniaturization comported the appearance of problems related to high heat-fluxes dissipation. In order to address such problems two-phase heat transfer devices are continuously under research and became a fundamental thermal management solution. In space applications, sintered wick heat pipes (HP) and Loop Heat Pipes (LHP) were developed because of their lightweight, reliability and capability of operation also without assistance of significant acceleration fields (Gilmore, 2002). This ability is obtained using a capillary structure which is also the most complex and expensive element inside the system. In a cost reduction perspective, Akachi (1990,1993) introduced the concept of Pulsating Heat Pipe (PHP), also known as Oscillating Heat Pipe (OHP), which is basically a wickless two phase loop, consisting of a capillary diameter tube bended in several turns so that the fluid resides inside the tube as an alternation of liquid slugs and vapor bubbles: when the vapor formed in the heated zone expands, it pushes the adjacent fluid to the condenser zone, where the heat is released and the vapor condenses. Generally, in the literature, the static criterion (Kew and Cornwell, 1998) is used to determine the critical tube diameter for capillarity. This criterion does not consider the fluid viscosity and inertia and is expressed as:

$$Bo = \frac{g(\rho_l - \rho_v)d^2}{\sigma} < 4 \quad (1)$$

Where  $Bo$  is the so-called Bond number,  $g$  is the gravity acceleration,  $\rho_l$  and  $\rho_v$  are respectively the liquid and

1 vapor densities,  $\sigma$  is the surface tension and  $d$  is the diameter of the tube. The criterion can be rewritten in the  
 2 expression for a critical diameter value as:

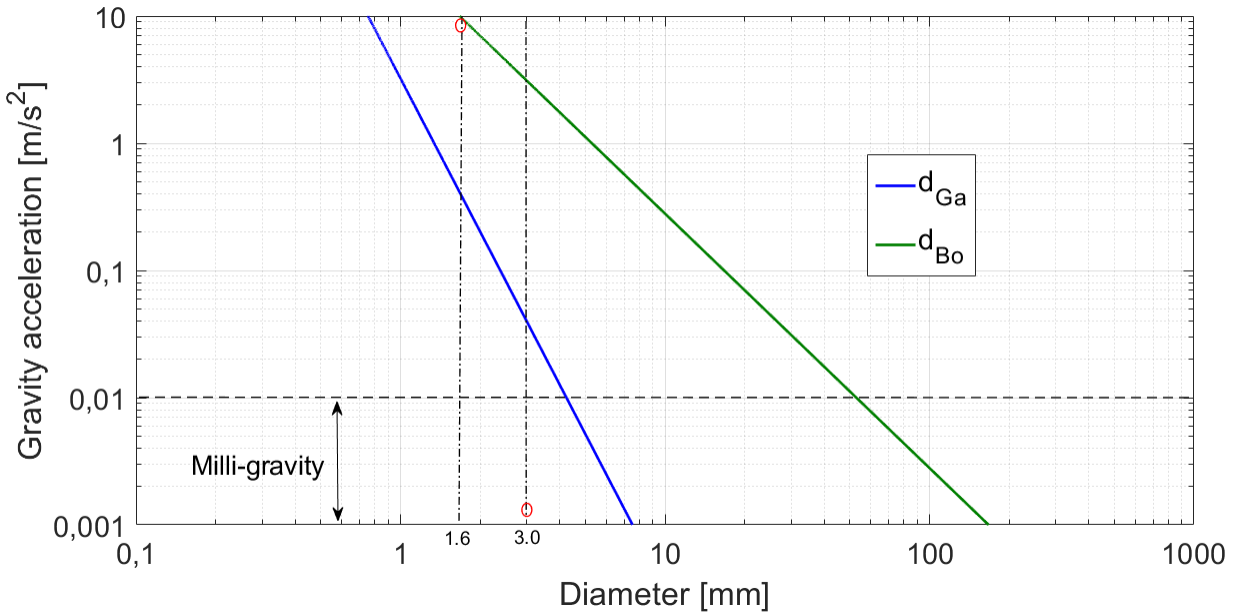
$$d_{cr} = 2 \sqrt{\frac{\sigma}{g(\rho_l - \rho_v)}} \quad (2)$$

3 From the simple formula shown, it seems evident that, as gravity decreases, bigger diameter of the tube could  
 4 be used still having a fluid motion governed by capillary forces. Gu et al. (2004, 2005) were the first to speculate  
 5 on the possibility to increase the PHP internal diameter improving the heat transfer capability. Indeed, in  
 6 microgravity conditions, the ratio between buoyancy forces and surface tension forces decreases allowing to  
 7 exploit larger diameter tubes with respect to the capillary limit on ground. However, the static criterion is not  
 8 accurately predictive for micro-gravity conditions where inertia and viscous effects play a significant role.  
 9 Baldassari and Marengo (2014) proposed a more comprehensive criterion based on the Garimella number:  
 10

$$Ga = \sqrt{Bo} Re_l < 160 \quad (3)$$

11 where  $Re_l = \rho_l U_l d / \mu_l$  is the Reynolds number of the liquid phase.

12 The static and dynamic critical diameters,  $d_{Bo}$  and  $d_{Ga}$ , are calculated according to both the criterions for  
 13  $C_6F_{14}$  at  $20^\circ C$ , considering a typical average velocity of the liquid phase equal to 0.1 m/s. Indeed, even considering  
 14 the most conservative criterion it should be theoretically possible to develop a two-phase loop working as a  
 15 Pulsating Heat Pipe (slug/plug flow pattern) even if the tube diameter is bigger than the critical value calculated in  
 16 ground conditions.



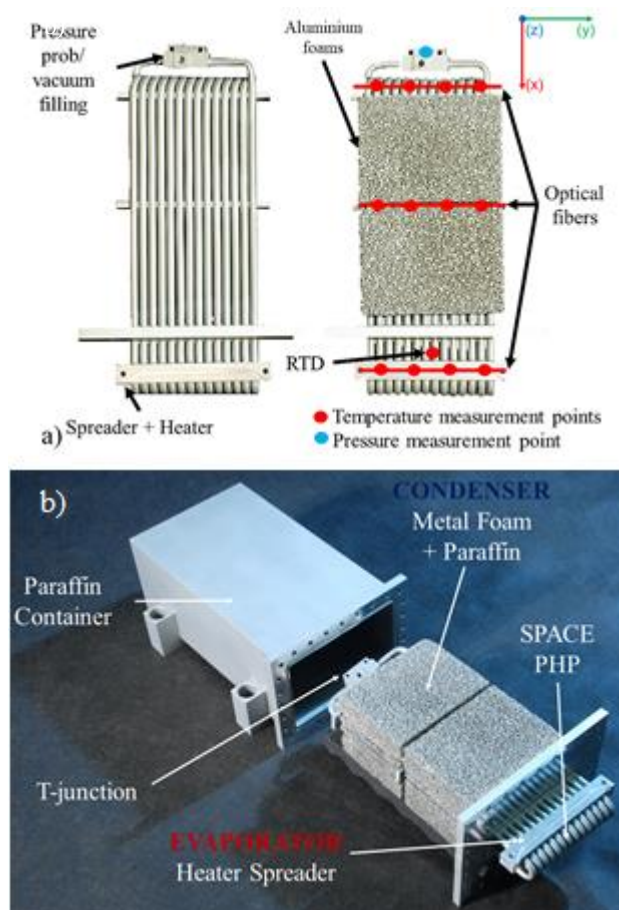
17 **Figure 1: Static and dynamic capillary limits for  $C_6F_{14}$  at  $20^\circ C$ , fluid velocity = 0.1 m/s.**  
 18

19 Many experiments in low gravity condition, i.e. by means of parabolic flight or sounding rockets, have been  
 20 carried out on capillary PHPs (Gu et al.2004, 2005; De Paiva et al. 2013, 2014; Mameli et al. 20140; Ayel et al.  
 21 2015; Taft et at. 20150). Most of them clearly revealed a self-sustained two-phase flow motion in micro-gravity,  
 22 while a few experiments have been performed when the tube diameter is bigger than the capillary limit on ground.  
 23 The Space PHP concept feasibility has been already successfully tested by Mangini et al. (2015, 2017), who tested  
 24 a PHP with an inner diameter of 3mm charged with  $C_6F_{14}$ , which is not capillary under normal gravity condition  
 25 (see Figure 1), both on ground and in milli-gravity condition during ESA 61 and 63 Parabolic flight campaign.

1 They noticed that a sudden transition of the flow pattern from stratified to slug flow takes place as the microgravity  
 2 occurs, showing that the device may work as a capillary tube PHP in such conditions. On ground the tube can  
 3 work as a two-phase loop thermosyphon. This concept of hybrid Loop Thermosyphon/Pulsating Heat Pipe  
 4 (LT/PHP) for space application was also tested by Ayel et al. (2016)0 in the flat plate configuration. The reduced  
 5 gravity ambient experienced in parabolic flight has a duration of about 20s, too short for reaching a steady state  
 6 condition and so characterize the thermal performance of the device. Due to that, the first experiment on the Space  
 7 PHP onboard a sounding rocket was performed in the REXUS 18 launch campaign, with the goal of obtaining  
 8 data on a longer microgravity duration (expected 120s) but it failed due to a problem in the rocket de-spinning  
 9 system (Creatini et. al, 2015). An updated version of the experiment was tested on board the REXUS 22 launch  
 10 campaign (Nannipieri et al. 2016, 2017). Here the results of the flight are compared to a post-flight ground test  
 11 campaign. The analysis sheds new light on the device startup phenomena and working regimes.

## 12 2 EXPERIMENTAL SETUP

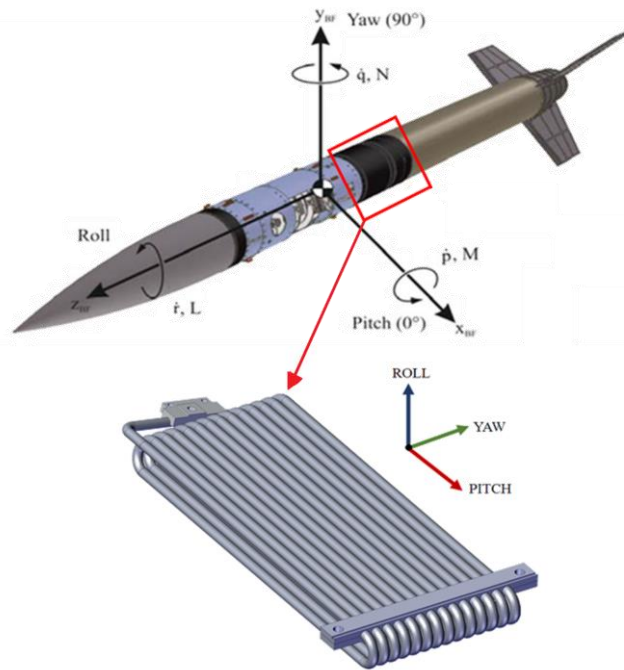
13 The Pulsating Heat Pipe is made of a 3 mm inner diameter aluminum tube (6060 alloy), arranged in a staggered  
 14 3D configuration with 14 turns at the evaporator as shown in Figure 2.



15  
 16 **Figure 2: a) test cell with measurement points description b) experiment box assembly.**

17 It is a closed loop, so the two ends of the tube are brazed on a T-junction that hosts the filling valve (Upchurch  
 18 Scientific® UP 447) and the pressure transducer (Kulite®, XCQ-093, 59,76 mV/bar, 850 Pa resolution) ports. The  
 19 device has been evacuated and then partially filled with the working fluid (perfluorhexane) at a volumetric ratio  
 20 of  $0,5 \pm 0,025$  (corresponding to 22 ml). The PHP condenser section is embedded into a heat sink, consisting of  
 21 an open cell metallic foam (ERG®, aluminum, 40 Pores Per Inch, 12% relative density) brazed on the PHP tubes  
 22 and filled with a Phase Change Material (PCM), octadecane paraffin wax. To avoid any leakage of the PCM, the  
 23 condenser section is contained inside an airtight box. Two flat ceramic heaters (Innovacera®, Electrical resistance

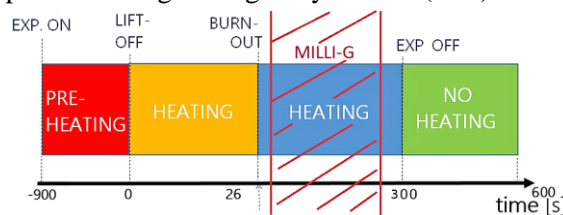
1 18 Ohms  $\pm 10\%$ ) are located on the evaporator zone to provide the heat power input, up to 200 W. The power is  
 2 supplied by a Li-ion battery pack (8s1p SAFT<sup>®</sup> Li-Ion cells, 28 V, 54.4 Ah) with high output current and regulated  
 3 by a VICor<sup>®</sup> DC-DC converter and controlled by a digital controller (Battery Management System, BMS in figure  
 4 1b). The test-cell is equipped with a Fiber Bragg Grating (FBG) temperature measurement system (SmartScan<sup>®</sup>  
 5 series realized by Smart Fibres<sup>®</sup> and Infibra Tec. <sup>®</sup>). It acquires temperatures in 24 points (12 on the upper side, as  
 6 shown in Figure 2a, and 12 below in the same positions) by means of optical sensors, with an accuracy of  $\pm 0.1$  K.  
 7 The accuracy of these novel sensors and their reduced amount of cabling (24 point of measure in 4 fibres) resulted  
 8 in a considerable upgrade with respect to the customary thermocouples. Up to the authors' knowledge, this is the  
 9 first time that this system is used to test a PHP and the first time on board a space vehicle as temperature sensor  
 10 (Nannipieri et al. 2017)0. Moreover, two class A Pt-100 ( $\pm 0.06 \Omega @ 0^\circ\text{C}$ ) are placed in the evaporator section for  
 11 FBG calibration and redundancy. Outputs coming from the optical sensors (at 10Hz), the pressure transducer (at  
 12 100Hz) and the g-sensor (at 10Hz) are recorded by a custom-made data handling system. Variable gravity levels  
 13 during the flight are detected by means of a three-axis g-sensor (Dimension Engineering<sup>®</sup>, DE-ACCM3d, sense  
 14 range:  $\pm 3g$ , sensitivity 333mV/g). This sensor is needed only to detect the switching from hyper gravity to  
 15 milligravity condition at burnout of the engine and the accelerations on the three axes (see Figure 3) when the de-  
 16 spin has taken place, thus the range is reduced to obtain better accuracy on acceleration levels when in milligravity.



17  
 18 **Figure 3: rocket body centered frame with description of axis orientation with respect to PHP position in the rocket.**

19 **2.1 Flight experimental procedure**

20 The overall experiment duration is 1200 s. Figure 4 shows the experiment timeline. Before the Lift Off (LO),  
 21 which is taken as a temporal reference point ( $t = 0s$ ), the rocket is standing on the launch pad in vertical position  
 22 and so the only acceleration component is the ground gravity in the z (Roll) direction (Figure 3).



23 **Figure 4: Experiment timeline.**  
 24

1 To set the heat sink temperature at 27°C (melting temperature of paraffin wax) a pre-heating phase is necessary  
 2 due to the cold temperatures typical of the launch location (Kiruna, Sweden) in March.

3 **Table 1: List of the launch events.**

Event	Time	Description
Start of Experiment	-900s	Ground g, Pre-Heating
Lift-Off	0s	~20 g , Regime Heating begins
Engine Burn-Out	26s	End of thrust
De-spin	65s	Start of Milli-g
End of Milli-g	~180s	Re-entry begins random accelerations
End of Experiment	~300s	Heating shut down. Send of backup data to ground

4 Therefore, the experiment is turned on at -900s. During this phase, the experiment performs a temperature  
 5 control to approach the PCM melting temperature. The amount of power supplied is depending on environmental  
 6 conditions and it can reach a peak of 200W. From the lift-off the PHP is heated with the maximum power of  
 7 200W. The rocket accelerating phase ends with the engine burn-out, which occurs at 26s after LO. At 65s the  
 8 payload de-spin occurs. The initial spin of the rocket is reduced to 0,04Hz. At this point micro-gravity conditions  
 9 are met and maintained for about 120s. After reaching its peak altitude, the payload starts the reentry phase and,  
 10 as soon as air density is high enough, the payload is subjected to the typical reentry conditions of a spacecraft: drag  
 11 forces are no more irrelevant and the micro-gravity phase ends. At 300s, the experiment is shut down and data are  
 12 sent to the control station for backup.

### 13 3 RESULTS

#### 14 3.1 Flight results

15 Results are shown in terms of temperature and fluid pressure temporal trends. The evaporator (red colors) and  
 16 the condenser (blue colors), as well as the fluid pressure are shown. To synchronize the gravity acceleration level  
 17 with the heat input power level and the data of interest during the flight, the temporal trends are shown as the  
 18 superposition of subplots. The acceleration field components (purple colors), the temperatures at the evaporator  
 19 (red colors) with the heat input power on the secondary axis (black color), the temperature at the condenser, (blue  
 20 colors), and finally the local condenser fluid pressure. In this way it is easy to relate the trends with the main  
 21 maneuvers, such as the lift off (LO), the despin (DS) and the end of microgravity conditions (EOg).

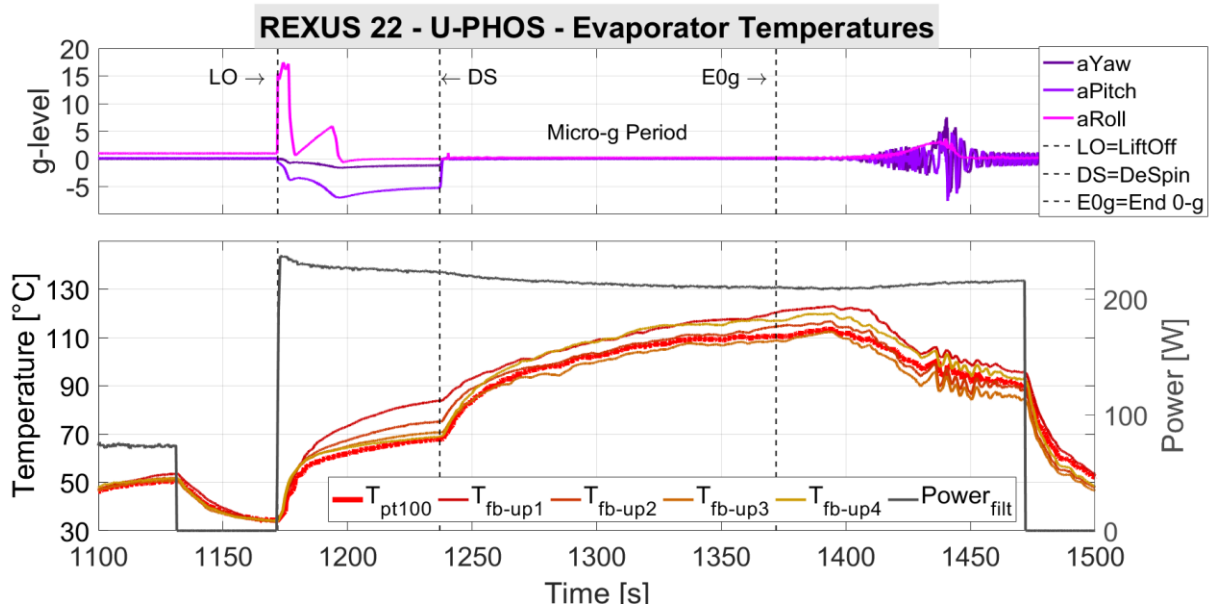


Figure 5: a) acceleration profile of the rocket; b) evaporator temperature trend

1 Before launch the device is heated up to maintain the PCM close to its melting point. The rocket is standing on  
 2 the launch-pad with a small inclination of few degrees. The PHP is placed inside the module so that the pre-heating  
 3 operation is aided by such orientation, activating a two-phase thermosyphon behavior and giving the possibility to  
 4 efficiently transfer heat to the condenser section and thus keep the paraffin wax in a proper range of temperature.  
 5 When Lift-Off occurs, the device is supplied with the maximum heating power input (~200 W, black signal in  
 6 Figures from 5 to 8), indeed both the evaporator and condenser temperatures rise. Between Lift-Off and De-Spin,  
 7 the rocket experiences nearly 20g acceleration in longitudinal direction (roll axis) due to the motor thrust and up  
 8 to 6g centrifugal component of acceleration (yaw and pitch) due to the rocket spinning. The first is perpendicular  
 9 to the flow path direction pushing the liquid phase once more in the lower tube rank; the second pushes the liquid  
 10 phase on the two ends of the device. The effect of this acceleration field on the thermo-fluidic behavior is  
 11 unpredictable but, on the overall, it is certainly assisting the fluid motion. After the rocket De-Spin, the three  
 12 acceleration components suddenly decrease, and the micro-gravity condition is reached.

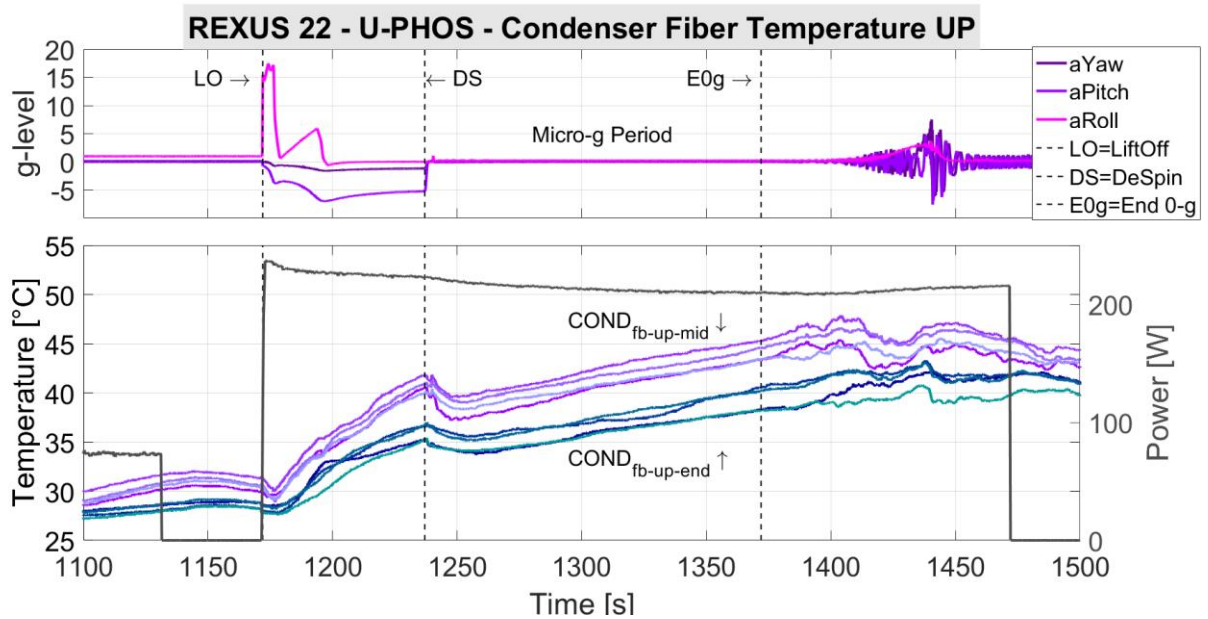


Figure 6: a) acceleration profile of the rocket; b) condenser temperature trend.

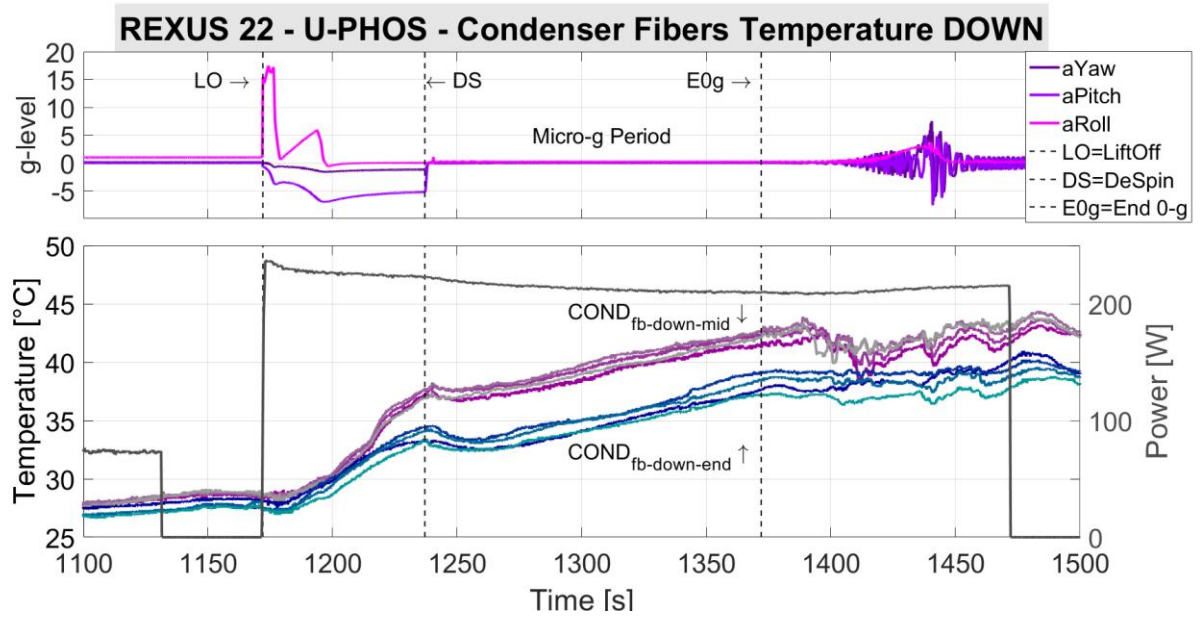
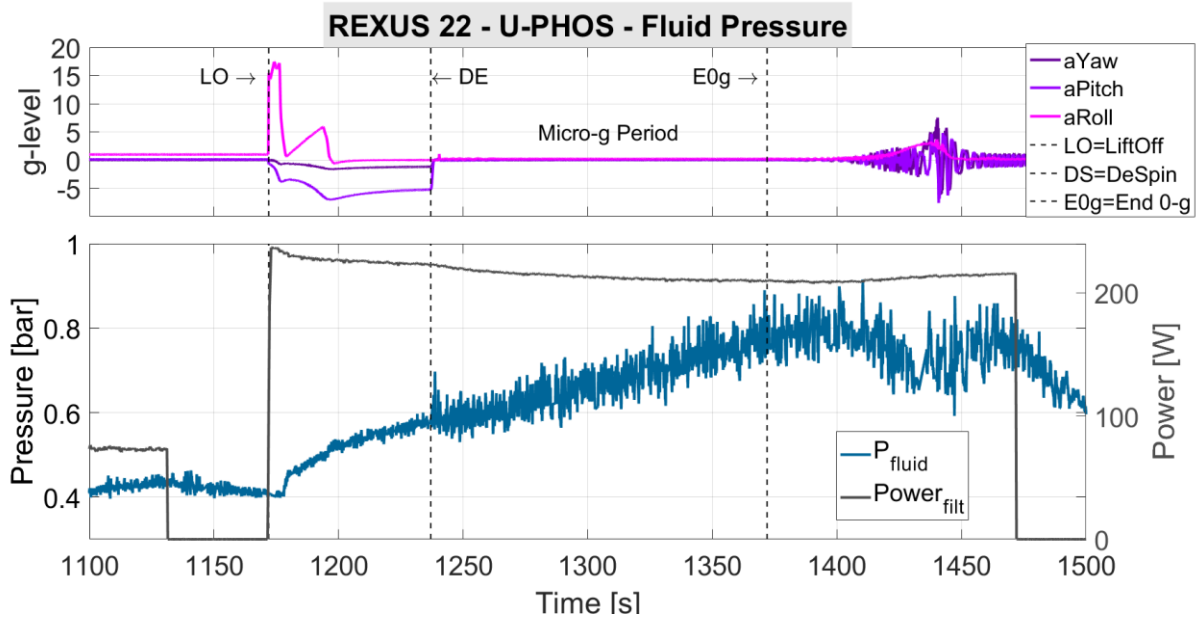


Figure 7: a) acceleration profile of the rocket; b) condenser furthest from evaporator temperature trend.

1 During this period, the fluid motion is only related to thermocapillary effects and the evaporator exhibits a  
 2 sudden increase, while the condenser temperature decreases meaning a sudden decrease of the overall heat transfer  
 3 performance with respect to the previous period.

4 It is reasonable to assess that the acceleration field during the launch phase has positive effect on the fluid  
 5 motion and consequently on the device heat transfer rate. Even if the device performance seems to degrade  
 6 during the milligravity period, both the temperature and fluid pressure trends show that the fluid motion is still  
 7 active inside the device. Temperatures both in the evaporator and condenser, as well as the fluid pressure  
 8 exhibit an oscillating component for the whole zero gravity duration and this is one the most important outcome  
 9 of the present work, since it basically confirms that a multi-turn two phase loop can work as a Space PHP in



**Figure 8: a) acceleration profile of the rocket; b) Local condenser fluid pressure**

10 microgravity conditions. It was not possible to reach a steady state probably because of the thermal inertia of  
 11 the heat sink. This confirms that, a longer-term micro gravity period is needed to infer about the actual heat  
 12 transfer performance.

13 With reference to Figure 8 is possible to distinguish different pressure behaviors during the flight. As long as  
 14 the preheating system is working, the evaporator temperature is indeed rising homogeneously, and the fluid  
 15 pressure signal is showing low amplitude oscillations due to white noise ( $\pm 500$  Pa). The fluid pressure signal  
 16 clearly reveals a change in the trend immediately after the occurring of the micro-gravity condition (DS in).  
 17 As the re-entry phase begins, the milli-gravity condition ends (E0g in the figures). In this period, the rocket  
 18 experiences a complex acceleration field that, once again unpredictably, assists the fluid motion: the evaporator  
 19 temperatures indeed decrease.

20 The Fluid pressure signal shown in Figure 8 clearly reveals a change in the trend immediately after the  
 21 occurring of milligravity. By matching the rocket flight results with the one obtained in microgravity conditions  
 22 during the 63<sup>rd</sup> Parabolic Flight Campaign by Mangini et al. (2015) on a very similar device with five U-turns at  
 23 the evaporator, same tube inner diameter (3mm), very similar working fluids (FC-72 and pure perfluorhexane),  
 24 same wall to fluid heat flux ( $12.5 \text{ W/cm}^2$ ), it can be noticed that the pressure absolute mean level and amplitude is  
 25 comparable (Figure 9). In particular, the pressure trend recorded during the parabolic flight exhibits a slightly  
 26 higher amplitude and it is characterized by some stop-over periods; interestingly the sounding rocket experiment  
 27 is characterized by a slightly lower amplitude without stop-over periods.

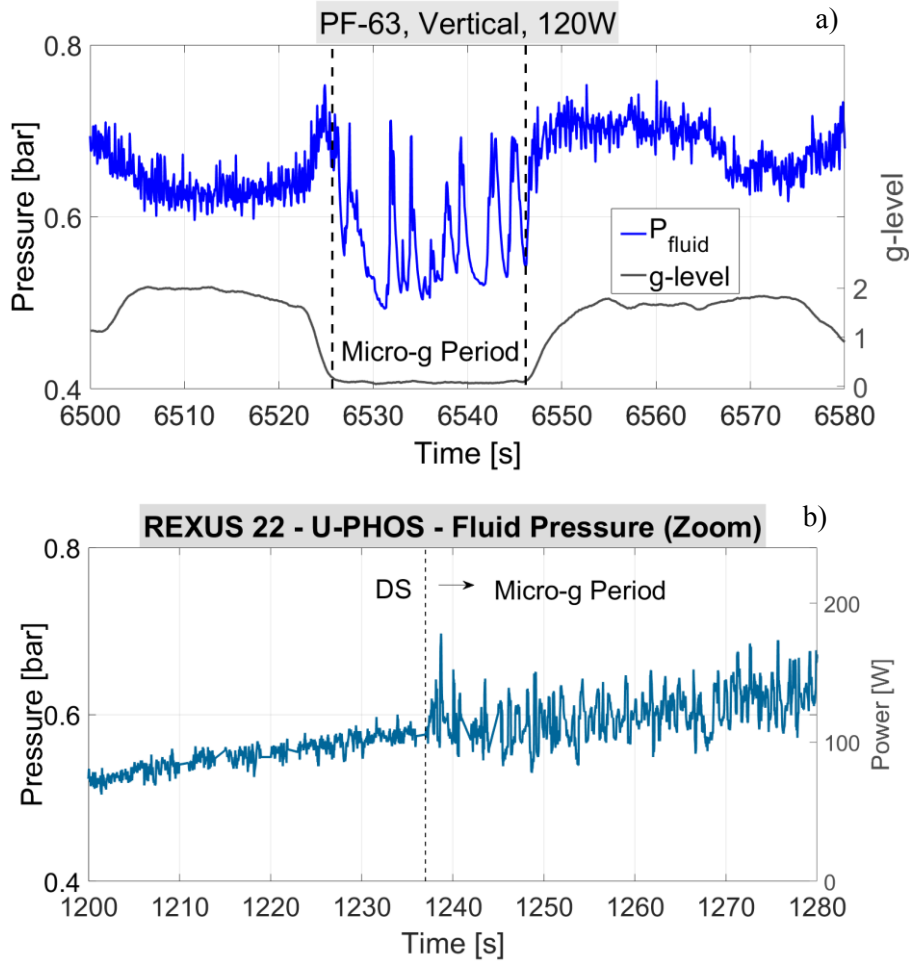


Figure 9: a) parabolic flight pressure signal; b) pressure variation at PHP activation during rocket launch

### 3.2 Ground tests results

It is worth reminding that the device is a hybrid between a multiple evaporator loop ThermoSyphon (TS) when gravity acceleration is present, and a Pulsating Heat Pipe (PHP) in low-gravity conditions as thoroughly explained by Mameli et al. (2016). For this reason, the ground campaign is devoted to compare the thermal behavior in TS mode (vertical, gravity assisted, Figure 10a), with the PHP mode (microgravity). Another term of comparison is the least efficient configuration: the horizontal position on ground shown in Figure 10b, which is not expected to work at all. However, tests have demonstrated that because of the 3D geometry, the fluid motion is activated also in horizontal and slight anti-gravity orientation and the device does not work at all only when  $\alpha = -25^\circ$ .

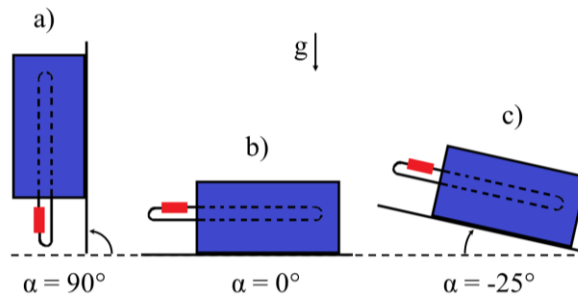
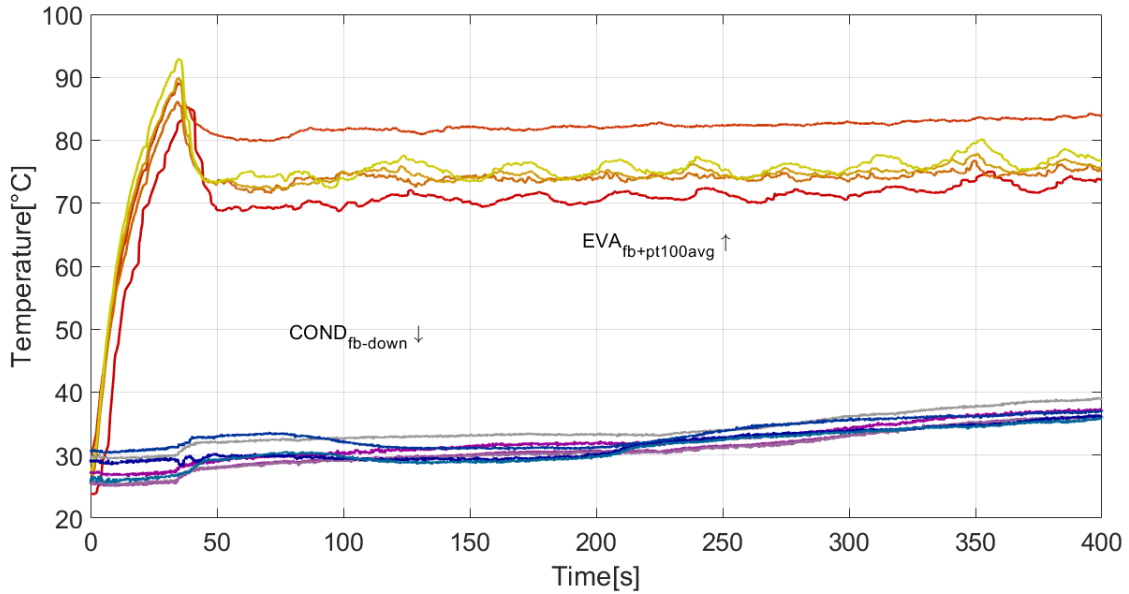


Figure 10: Ground tests orientations with respect to gravity direction a) vertical bottom heated, b) horizontal, c)  $25^\circ$  inclination, upper heated mode.

1 Long-run ground tests are performed, to reach a complete steady state of the device at the same heat input level  
2 used for the flight test.



**Figure 11: Ground bottom heated vertical test result, at 200W power input**

3 Figure 11 shows the behavior of the device tested on ground in vertical bottom heated mode. The typical  
4 thermosyphon behavior is detectable: in this condition the surface tension forces are not able to overcome the

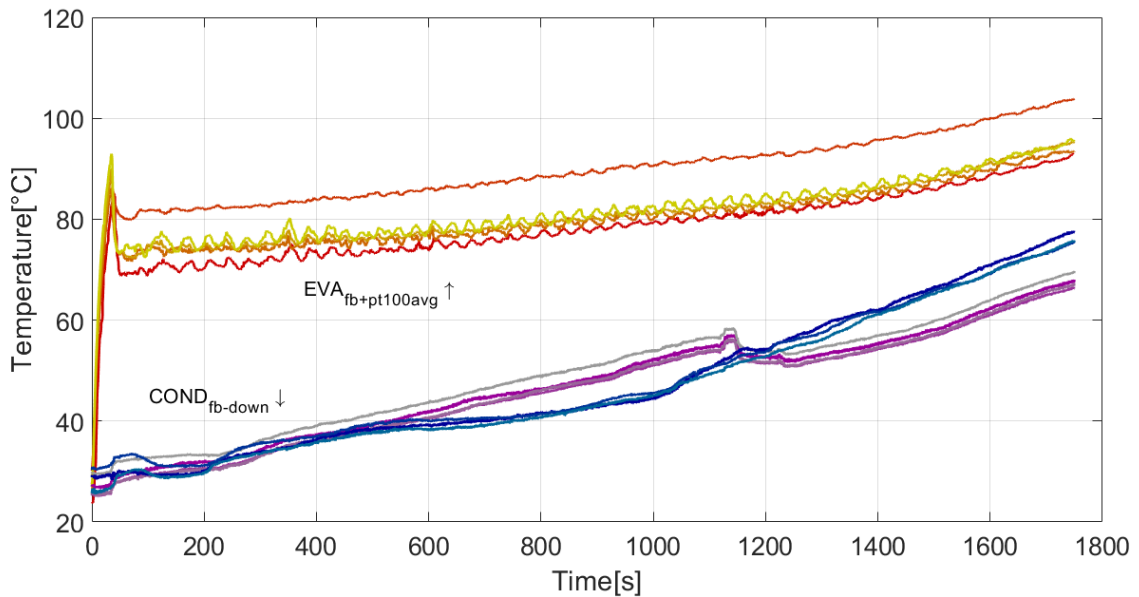


**Figure 12: Long run of the bottom heated vertical test**

5 buoyancy, thus the liquid phase initially wets the whole bottom part (evaporator) while vapor phase accumulates  
6 in the higher part (condenser section). The liquid phase boils continuously and the generated vapor rises towards  
7 the condenser dragging liquid batches in the so-called "bubble lift" mode. Figure 12 highlights that the PCM- metal  
8 foam heat sink is not the best way to dissipate the amount of heat supplied during long run tests. After about 20  
9 min there is a sensible increment in both the evaporator and condenser temperatures. This happens because of the  
10 complete paraffin wax melting, which prevents the possibility to further absorb heat via latent heat of fusion.  
11

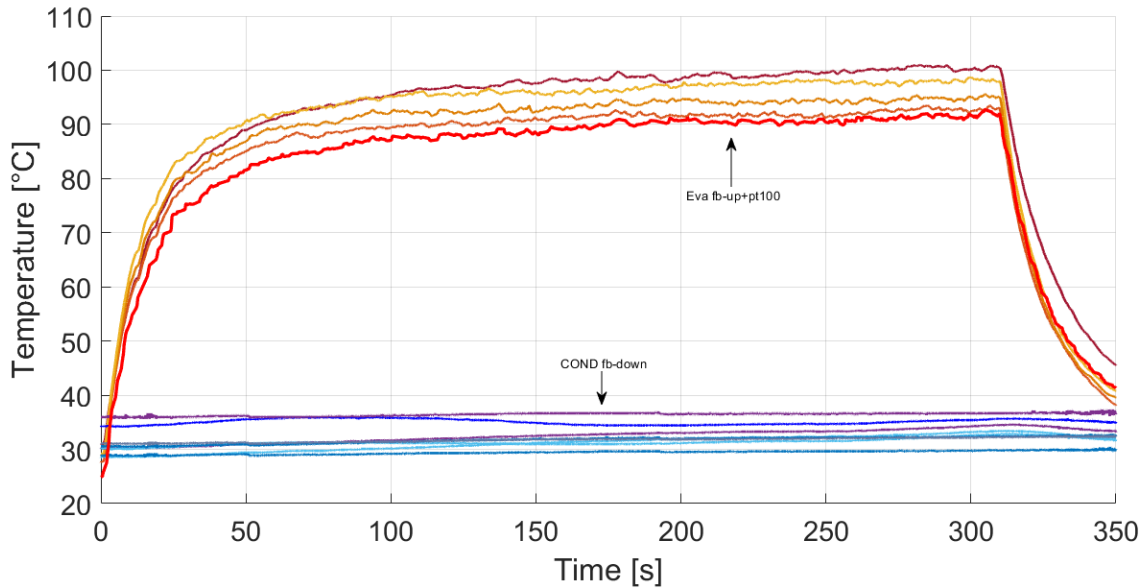


Figure 13: Ground horizontal test at 200W.

In Figure 13 is shown the temperature trend of an horizontal position test. It is possible to understand that, differently from what expected, the device still activates as a two-phase thermosyphon. Figure 14 shows the temperature temporal evolution in the case of slight anti-gravity inclination ( $\alpha = -25^\circ$ ) of the evaporator with respect to the condenser. Being the internal tube diameter bigger than the critical one on ground, no capillary fluid motion is activated because of the two-phase fluid stratification, so the liquid phase resides in the lower tube rank and heat is only transferred by means of conduction. The experiment is shut down by the safety thermal switches before reaching the steady state due to the high temperatures.

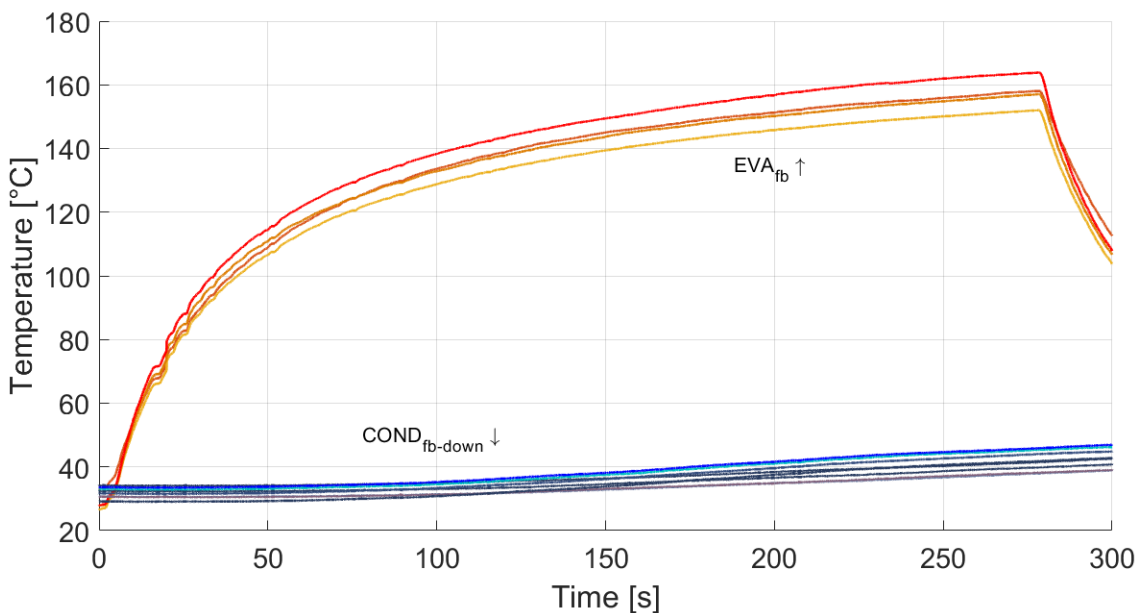
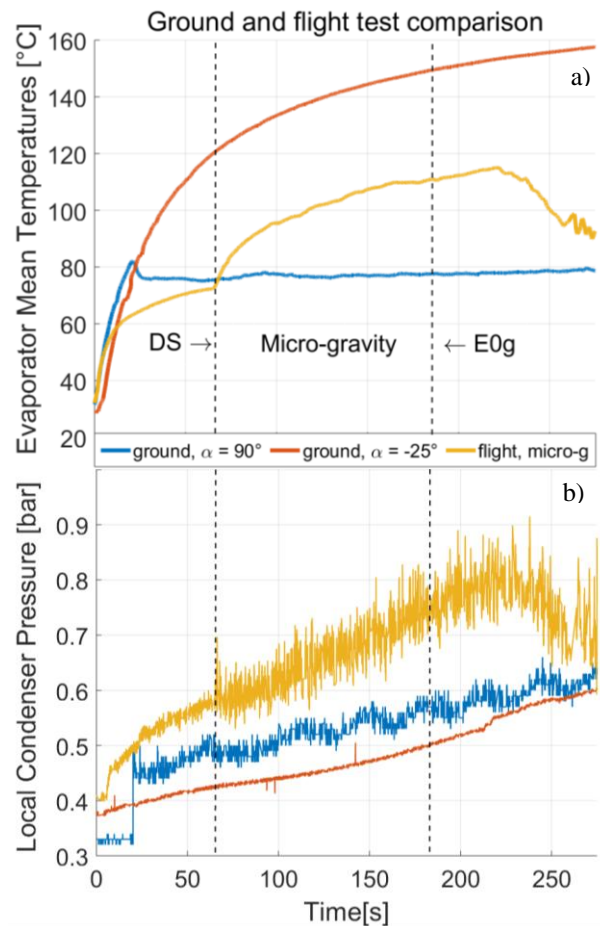


Figure 14: Temperature trend of the ground test upper heated mode.

### 3.3 Comparison

The comparison between flight and ground data focuses on the startup phenomena during the transient time. Figure 15 shows the comparison between the evaporator arithmetic average temperature and the local condenser fluid pressure for three reference cases: ground vertical (TS bottom heated, blue line), flight (PHP mode in microgravity, yellow line) and finally, ground  $\alpha = -25^\circ$ , (TS slight anti-gravity). This shows where the PHP mode

1 resides with respect to the two extreme cases of the TS mode, namely the vertical-high performance gravity  
 2 assisted mode and the slight anti-gravity mode where there is no pressure oscillations (Figure 15b) and very likely  
 3 no fluid motion, and the heat is transferred only by conduction. At  $t=0$ s the heat input is supplied for the three tests.  
 4 The ground vertical case could reach a steady state, while for the flight test, as soon as the micro-g condition is  
 5 reached, the behavior suddenly changes, with a new transient period associated to the operational transition from  
 6 TS to PHP mode. Despite the PHP mode seems not to perform as good as the TS vertical mode, the device is very  
 7 close to reach a pseudo steady state and set to pretty much lower temperatures with respect to the purely conductive  
 8 medium.



9  
 10 **Figure 15: a) Comparison of evaporator temperature among ground and flight tests b) Comparison of pressure**  
 11 **signals.**

## 12 4 CONCLUSION

13 The U-PHOS Project aims at characterizing the thermal behaviour of a large diameter Pulsating Heat Pipe  
 14 (Hybrid TS/PHP), a promising device for thermal management for ground and space applications. The  
 15 experiment is an upgrade of a previous experiment (PHOS), which was launched on board REXUS 18  
 16 sounding rocket. The main novelties with respect to PHOS consist of a new optimized staggered geometry of  
 17 the tube, the enhancement of the heat sink thermal conductivity using a metal foam directly brazed on the PHP  
 18 tubes and filled with a paraffin wax. Important technological advancement is given by the implementation of  
 19 a temperature measurement system based on optical fibres, which proved to be accurate, reliable and easy to  
 20 embed. Ground tests confirmed that the device successfully works as a gravity assisted two-phase loop  
 21 thermosyphon. Still, due to the 3D configuration, the device works in the horizontal position too and a slight  
 22 antigravity ( $\alpha = -25^\circ$ ) inclination is needed to inhibit the fluid motion and analyse the purely conductive mode.

1 The experiment has been successfully tested in micro-gravity condition, on board REXUS 22 sounding rocket  
 2 in March 2017. At the occurring of the micro-gravity period, all the temperature signals both in the evaporator  
 3 and condenser exhibit an oscillating behavior for the whole low gravity duration.

4 Differently from similar experiments in the literature, the fluid local pressure trend is not characterized by  
 5 stop-over phenomena.

6 The device is very close to reach a pseudo-steady state and set to higher temperatures with respect to the vertical  
 7 TS mode but also to pretty much lower temperatures with respect to the purely conductive medium. This  
 8 emphasizes the fact that a longer micro-gravity period is needed to measure the potential heat transfer performance.

9 **ACKNOWLEDGMENTS**

10 The present work has been carried out as part of the REXUS BEXUS program, supported by European  
 11 space agency (ESA), German Aerospace Research Establishment (DLR) and Swedish National Space Board  
 12 (SNSB). The ESA MAP INWIP project for funding the project, the International Scientific Team on Pulsating  
 13 Heat Pipes, the school of engineering and all the technical sponsors  
 14 (<http://www.uphos.ing.unipi.it/it/supporters/>). Thanks to Roberto Manetti, Massimo Ciampalini, Franco  
 15 Peticca, Davide Della Vista for their essential technical contribution. The authors would like to thank the  
 16 Alessandro Signorini and INFIBRA Technology for the great help.

17 **NOMENCLATURE**

<b>Variable</b>	<b>Description</b>	<b>Unit</b>
<i>Bo</i>	Bond Number	[-]
<i>d</i>	Diameter	[m]
<i>g</i>	Gravity Acceleration	[m/s <sup>2</sup> ]
<i>Ga</i>	Garimella Number	[-]
Re	Reynolds Number	[-]
<i>T</i>	Temperature	[°C]
U	Velocity	[m/s]
$\mu$	Dynamic Viscosity	[Pa·s]
$\rho$	Density	[kg/m <sup>3</sup> ]
$\sigma$	Tension Surface	[N/m]

18 **Subscripts**

<b>Variable</b>	<b>Description</b>
<i>Bo</i>	Bond Number
cr	Critical
<i>Ga</i>	Garimella Number
<i>l</i>	Liquid Phase
<i>v</i>	Vapor Phase

## 1 REFERENCES

- 2 Gilmore, D. G., *Spacecraft Control Handbook, Fundamental Technologies, Second Edition, Vol. 1, The Aerospace Corp.,*  
3 *AIAA Publ., (2002).*
- 4 Akachi H., 1990. Structure of a heat pipe, *US Patent 4.921.041.*
- 5 Akachi H., 1993. Structure of a micro heat pipe, *US Patent 5.219.020.*
- 6 Kew, P.A. and K. Cornwell, Correlations for the prediction of boiling heat transfer in small-diameter channels”. *Applied*  
7 *Thermal Engineering, Vol. 17, pp. 705–715, (1997).*
- 8 Gu, J., Kawaji, M., Futamata, R., Effects of gravity on the performance of pulsating heat pipes, *J. Thermophys. Heat Trans.*  
9 *Vol. 18, pp. 370–378 (2004).*
- 10 Gu, J., Kawaji, M., Futamata, R., Microgravity performance of micro pulsating heating pipe, *Micrograv. Sci. Technol. Vol.*  
11 *16, pp. 179–183 (2005).*
- 12 Baldassari, C., Marengo, M. Flow boiling in microchannels and microgravity. *Prog. Energy Combust. Sci., Vol. 39, pp. 1-36*  
13 *(2013).*
- 14 De Paiva, K.V., Mantelli, M.B.H., Slongo, L.K., Burg, S.J., Experimental tests of mini heat pipe, pulsating heat pipe and heat  
15 spreader under microgravity conditions aboard suborbital rockets, *Proc. of the 15th IHPC, Clemson, South Carolina, USA,*  
16 *2010.*
- 17 De Paiva, K.V., Mantelli, M.B.H., Florez, J.P.M., Nuernberg, G.G.V., Mini heat pipe experiments under microgravity  
18 conditions. What have we learned? *Proc. of the 17th IHPC, Kanpur, India, 2013.*
- 19 Mameli, M., Araneo, L., Filippeschi, S., Marelli, M., Testa, R., Marengo, M., Thermal performance of a closed loop pulsating  
20 heat pipe under a variable gravity force, *Int. J. Ther. Sci., Vol. 80, pp.11–22 (2014).*
- 21 Ayel, V., Araneo, L., Scalambra, A., Mameli, M., Romestant, C., Piteau, A., Marengo, M., Filippeschi, S. Bertin, Y.,  
22 Experimental study of a closed loop flat plate pulsating heat pipe under a varying gravity force, *Int. J. Therm. Sci., Vol.*  
23 *96, pp. 23–34 (2015).*
- 24 Taft, B.S., Laun, F.F., Smith, S., Microgravity performance of a structurally embedded oscillating heat pipe, *J. Thermophys.*  
25 *Heat Transfer, Vol. 29 (2), (2015).*
- 26 Mangini, D., Mameli, M., Geourgoulas, A., Araneo, L., Filippeschi, S., Marengo, M., A pulsating heat pipe for space  
27 applications: ground and microgravity experiments, *Int. J. Therm. Sci. Vol. 95, pp. 53–63 (2015).*
- 28 Mangini, D., Mameli, M., Fioriti D., Araneo L., Filippeschi S., Marengo M., Hybrid Pulsating Heat Pipe for Space  
29 Applications with Non-Uniform Heating Patterns: Ground and Microgravity Experiments, *App. Therm. Eng. Vol. 126 pp.*  
30 *1029–1043 (2017).*
- 31 Ayel, V., Araneo, L., Marzorati, P., Romestant, A., Bertin, Y., Marengo, M., Visualization of Flow Patterns in Closed Loop  
32 Flat Plate Pulsating Heat Pipe Acting as Hybrid Thermosyphons under Various Gravity Levels, *Heat Transfer Engineering,*  
33 *(2018), In press, DOI: 10.1080/01457632.2018.1426244.*
- 34 Creatini F., Guidi G.M., Belfi F., Cicero G., Fioriti D., Di Prizio D., Piacquadio S., Becatti G., Orlandini G., Frigerio A.,  
35 Fontanesi S., Nannipieri P., Rognini M., Morganti N., Filippeschi S., Di Marco P., Fanucci L., Baronti F., Manzoni M.,  
36 Mameli M., Marengo M., 2015. “Pulsating Heat Pipe Only for Space: Results of the REXUS 18 Sounding Rocket  
37 Campaign”, XXXIII UIT Congress, L’Aquila, Italy, *Journal of Physics: Conference Series 655 (2015) 012042.*
- 38 Nannipieri P., Anichini M., Barsocchi L, Becatti G., Buoni L., Celi F., Catarsi A., Di Giorgio P., Fattibene P. Ferrato E.,  
39 Guardati P., Mancini E., Meoni G., Nesti F., Piacquadio S., Pratelli E., Quadrelli L., Viglione A. S., Zanaboni F., Mameli  
40 M., Baronti F., Fanucci L., Marcuccio S., Bartoli C., Di Marco P., Bianco N., Marengo M., Filippeschi S., 2016. “U-PHOS  
41 Project: Development of a Large Diameter Pulsating Heat Pipe Experiment on board REXUS 22”, 34th UIT Conference  
42 4-6 July 2016, Ferrara, Italy.
- 43 Nannipieri P., Anichini M., Barsocchi L, Becatti G., Buoni L., Celi F., Catarsi A., Di Giorgio P., Fattibene P. Ferrato E.,  
44 Guardati P., Mancini E., Meoni G., Nesti F., Piacquadio S., Pratelli E., Quadrelli L., Viglione A. S., Zanaboni F., Mameli  
45 M., Baronti F., Fanucci L., Marcuccio S., Bartoli C., Di Marco P., Bianco N., Marengo M., Filippeschi S., 2017. “The U-  
46 PHOS experience within the ESA studentREXUS/BEXUS programme: a real space hands-on opportunity”, IEEE  
47 EDUCON Conference 2017.
- 48 Nannipieri P., Anichini M., Barsocchi L, Becatti G., Buoni L., Celi F., Catarsi A., Di Giorgio P., Fattibene P. Ferrato E.,  
49 Guardati P., Mancini E., Meoni G., Nesti F., Piacquadio S., Pratelli E., Quadrelli L., Viglione A. S., Zanaboni F., Mameli  
50 M., Baronti F., Fanucci L., Marcuccio S., Bartoli C., Di Marco P., Bianco N., Marengo M., Filippeschi S., Upgraded  
51 Pulsating Heat Pipe Only For Space (U-Phos): Results Of The 22nd Rexus Sounding Rocket Campaign, *9th ExHFT, 12-*  
52 *15 June, 2017, Iguazu Falls, Brazil.*

- 1 Nannipieri, P., Meoni, G., Nesti, F., Mancini, E., Celi, F., Quadrelli, L., Ferrato, E., Guardati, P., Baronti, F., Fanucci, L.,  
2 Signorini, A., Nannipieri, T., Application of FBG sensors to temperature measurement on board of the REXUS 22  
3 sounding rocket in the framework of the U-PHOS project, 4th IEEE International Workshop on Metrology for AeroSpace,  
4 MetroAeroSpace 2017; Padua; Italy; 21 -23 June 2017.
- 5 Mamei M., Mangini D., Vanoli G., Filippeschi S., Araneo L., Marengo M., Advanced Multi-Evaporator Loop Thermo-  
6 syphon, *Energy*, Vol. 112, pp. 562–573, (2016).